CrossMark

RESEARCH ARTICLE

Source apportionment of polycyclic aromatic carbons (PAHs) in sediment core from Honghu Lake, central China: comparison study of three receptor models

Huang Zheng[1] · Dan Yang[2] · Tianpeng Hu[1] · Ying Li[1] · Gehao Zhu[1] · Xinli Xing[1,3] · Shihua Qi[1,3]

Abstract The spatial distribution of polycyclic aromatic hydrocarbons (PAHs) and their source contributions employing receptor models has been widely reported. However, the temporal distribution of PAH source contributions is less studied. Thus, in this paper, three receptor models including principle component analysis-multiple linear regression (PCA-MLR), positive matrix factorization (PMF), and Unmix were used to PAH source apportionment study in a sediment core from Honghu Lake, China. Sixteen USEPA priority PAHs in 37 sliced sediment layers (1-cm interval) were measured, with the concentrations of $\sum_{16}$PAH (sum of 16 PAHs) ranging from 93.0 to 431 ng g^{-1}. The source apportionment results derived from three receptor models were similar, with three common sources: mixed sources of biomass burning and coal combustion (31.0–41.4% on average), petroleum combustion (31.8–45.5%), and oil leakage (13.1–21.3%). The PMF model segregated an additional source: domestic coal combustion (contributed 20.9% to the $\sum_{16}$PAHs). Four aspects including intra-comparison, inter-comparison, source numbers and compositions, and source contributions were considered in comparison study. The results indicated that the PMF model was most reasonable in PAH source apportionment research in this study.

Introduction

It is generally known that polycyclic aromatic hydrocarbons (PAHs) are both from natural (Readman et al. 2002; Micić et al. 2011) and anthropogenic sources (Larsen and Baker 2003; Huang et al. 2012), and they have been found in various environmental medias (Larsen and Baker 2003; Ma et al. 2010; Zhang et al. 2012; Yang et al. 2013a). PAHs originated from anthropogenic activities including coal combustion, oil spill, vehicular emission, and industrial discharge (Stout and Graan 2010). These activities are thought to be the main sources of PAHs in the environment (Zakaria et al. 2002). In the aquatic environment, petrogenic PAHs are usually introduced directly into the water body, while pyrogenic PAHs are first emitted into the air and subsequently settled down into the water body and ultimately the sediments. The contents and compositions of the PAHs in sediment varied at different times resulting in temporal distribution, which revealed the anthropogenic impacts and economic development (Guo et al. 2010; Liu et al. 2012). Therefore, the dated sediment cores are good archives to reconstruct the chronology of PAHs in the aquatic system (Guo et al. 2006; Lin et al. 2012; Xu et al. 2014).

Several studies have identified the possible sources of PAHs in the sediment core employing diagnostic ratios and receptor models (Guo et al. 2006; Guo et al. 2010; Wang et al. 2010). The source category of PAHs can be qualitatively identified using PAH isomeric ratio methods. For receptor models,

✉ Dan Yang
   yangdan322@139.com

1   School of Environmental Studies, China University of Geosciences, Wuhan 430074, China

2   Faculty of Engineering, China University of Geosciences, Wuhan 430074, China

3   State Key Laboratory of Biogeology and Environmental Geology, China University of Geosciences, Wuhan 430074, China

however, the source category and contribution can be quanti-tatively apportioned (Feng et al. 2007; Malik et al. 2011). Three commonly applied receptor models without employing source profile data are principle component analysis-multiple linear regression (PCA-MLR) (Bzdusek et al. 2004; Shi et al. 2009; Hu et al. 2017), positive matrix factorization (PMF) (Sofowote et al. 2011; Zhang et al. 2012; Yang et al. 2013b), and Unmix (Henry 1997; Yang et al. 2013a; Lang and Yang 2013). These source unknown receptor models have been widely used to source apportionment studies. Although these models aim at source apportionment, they differ to each other in mechanisms. The target of PCA-MLR is dimension reduc-tion and explains the dataset with smaller number of indepen-dent factors, while PMF makes full use of available data to retain missing and below detection limit values and estimates the confidence of each input value. Unmix reduces the dimen-sionality of data using a singular value decomposition (SVD) (Henry 2003). PMF and Unmix are originally developed to identify and quantify the source of air pollutants including particulate matters and volatile organic hydrocarbons. In recent years, these receptor models are applied to PAH source apportionment in surface sediments. For example, Zhang et al. (2012) utilized these three models to study the spatial distribution of PAH source contributions and risk as-sessment in sediment from Taihu Lake, China. Similar studies applying the receptor model to investigate the spatial distribu-tion of PAH sources and risk in surface sediments can be found elsewhere (Yu et al. 2015; Xu et al. 2016). Inspired by these studies, the goal of figuring out the historical distribution of PAH source contributions could be achieved by the receptor models and dated sediment core.

Honghu Lake, the largest freshwater lake in Hubei province, was chosen as the study area for its significant values in agricul-ture, ecology, and flood control. In this study, 16 USEPA priority PAHs in each layer were determined. The potential sources and average contributions were apportioned utilizing PCA-MLR, PMF, and Unmix models. Furthermore, the comparison study of three different receptor models was conducted through (1) the fitting degrees between the observed and predicted (O/P) PAH concentrations, (2) inter-comparison of different models, (3) source numbers and compositions, and (4) the historical distri-bution of each source to the total concentrations. Results of this study could provide the information about the historical varia-tion of PAH source contribution in Honghu Lake and contributed to developing the countermeasures of PAH control.

Materials and methods

Field works

A sediment core (φ 100 mm × 37 cm) was collected in the central area of Honghu Lake (Fig. S1) with the help of a gravity

corer in December 2014. The sediment core was sliced into a 1-cm interval, wrapped in acetone-cleaned aluminum foil, and transported to the laboratory in an ice cooler. The sediment samples were stored at − 20 °C until further treatment.

PAH analysis

The detailed PAH analysis procedure was reported elsewhere (Grimalt et al. 2004). Briefly, approximately 3–5 g freeze-dried, homogenized sediment sample spiked with surrogate (mixture of five deuterated PAHs: naphthalene-d8, acenaphthene-d10, phenanthrene-d10, chrysene-d12, and perylene-d10) was ultrasonic extracted with 1:1 (v/v) dichloromethane-acetone (3 × 20 mL, 15 min). A rotary evap-orator was used to concentrate the extract to 10 mL, and hy-drolyzation was operated by adding an extra 20 mL KOH in methanol (6%, w/w). The neutral fractions were recovered with 30 mL hexane (3 × 10 mL), vacuum evaporated to almost dryness, and fractionated using a column filled with alumina-silica (1:1, v/v). PAH fractions were eluted by 15 mL dichloromethane-hexane (2:1, v/v). High-purified (> 99.999%) N_2 was used to concentrate target elutes (PAHs fractions) to 0.2 mL. Prior to GC/MS analysis, 1000 ng inter-nal standard (hexamethylbenzene) was spiked.

Sixteen US EPA priority PAHs—naphthalene (Nap), ace-naphthylene (Acy), acenaphthene (Ace), fluorene (Fl), phen-anthrene (Phe), anthracene (Ant), fluoranthene (Fla), pyrene (Pyr), benz[a]anthracene (BaA), chrysene (Chr), benzo[b]fluoranthene (BbF), benzo[k]fluoranthene (BkF), benzo[a]pyrene (BaP), indeno[1,2,3-cd] pyrene (IcdP), dibenz[a,h]anthracene (DBA), and benzo[ghi]perylene (BghiP)—were analyzed. Samples (1 μL) were injected (splitless mode) into an Agilent GC (6890N) coupled with DB-5MS capillary column (30 m, 0.25 mm ID, 0.25 μm film) to separate PAHs with helium carrier gas at a constant flow of 1 mL min^{-1} and programmed temperature of the GC oven: initially 50 °C holding for 2 min, 20 °C min^{-1} to 180 °C and 4 °C min^{-1} to 250 °C and 10 °C min^{-1} to 300 °C min^{-1} and holding for 5 min. An Agilent MS (5975) with EI source (70 eV) operated in selected ion monitoring (SIM) mode was used to analyze PAHs. Injector and mass transfer line temperatures were held at 280 °C.

The procedural blank, blank-spiked, matrix-spiked, and duplicated samples were processed in every 10 field samples for quality assurance (QA) and quality control (QC). Surrogate standard recoveries for QA/QC samples were 88 ± 11, 84 ± 38, 95 ± 38, 95 ± 14, and 92 ± 22% for naph-thalene-d8, acenaphthene-d10, phenanthrene-d10, chrysene-d12, and perylene-d12, respectively. Recoveries of the same surrogate standards for field samples were 79 ± 16, 93 ± 13, 102 ± 23, 89 ± 13, and 84 ± 22%, respectively. Three times of the signal-to-noise level in the lowest standard sample con-centration (0.2 mg mL^{-1}) was defined as instrument detection

limit (IDL) and ranged from 0.10 to 0.73 mg L^{-1} (Table S1, supplementary materials). All concentrations were reported after normalized to dry weight, and blank corrected but not surrogated recovery corrected (Zhang et al. 2013).

Receptor model description

Receptor models use statistical or mathematical methods to identify and quantify the source of pollutants at receptor samples. Unlike the dispersion models such as backward trajectory and photochemical models, receptor models do not use the meteorological data and chemical transformation mechanisms. Instead, the PCA-MLR, PMF, and Unmix models generate possible "candidate" source fingerprints, and then identify the source profile by comparing them with the known source profiles. Usually, these receptor models can be expressed as the following equation (Hopke 2003):

$$x_{ij} = \sum_{k=1}^{p} g_{ip} f_{pj} + e_{ij} \tag{1}$$

where x_{ij} is the jth compound concentration measured in the ith receptor sample; g_{ip} is the contribution of the pth source to the ith sample; f_{pj} is the concentration of the jth compound in the pth source; and e_{ij} is the error.

PCA-MLR

The SPSS (22.0, IBM USA) software was used to run the PCA-MLR. The dimension reduction of a matrix (37×16) was conducted using the factor analysis. The principle component method was used to extract the factors based on eigenvalues > 1. The Varimax rotation was also applied to make the factor loading values more physically interpretable. The Kaiser-Meyer-Olkin and Bartlett's test of sphericity results indicated that the raw data was suitable to employ the factor analysis model (Table S2). To calculate the contribution of each factor, multiple linear regression analysis was performed on the PCA score. More details can be found in the researches of Larsen and Baker (2003) and Cao et al. (2011).

PMF

The concentration file (a dataset of 37×16) and uncertainty file (equation based) were introduced into the PMF 3.0 model (https://www.epa.gov/air-research/positive-matrix-factorization-model-environmental-data-analyses). The 16 species were firstly categorized to strong due to the signal-to-noise ratio (S/N) higher than 2. A base run was conducted, starting a random seed for each iteration in each run of 20 times. After the first base run, Nap, Acy, Fl, Ant, and Pyr were categorized to weak for their residuals greater than ± 3 standard deviation (Fig. S2). Modified species categories were re-run to find the optimum factor numbers. The sixth run for four

factors reached the lowest Q_{true} value (the goodness-of-fit parameter calculated including all data) being 374.8, which was close to the $Q_{theoretical}$ value (380, $i \times j - p \times (i + j)$). Besides, the correlation between observed PAH concentrations and predicted values performed by PMF was significant with $r = 1.00$ ($p < 0.01$). After the four-factor solution considered as the local minima, bootstrap runs and F-peak (0.7) techniques were performed to estimate the stability and uncertainty of the solution and examine the rational ambiguity, respectively. More information about the PMF operation can be found elsewhere (USEPA 2008).

Unmix

Unmix is also one of the recommended receptor models by USEPA and available at https://www.epa.gov/air-research/unmix-60-model-environmental-data-analyses. Different from the PMF model input files, only concentration data were introduced into Unmix 6.0 software. No species were excluded in the model after evaluating the noise of species using the suggested exclusion function. The dataset of fitting PAH species was used in factor analysis to determine the source numbers. Three sources (factors) were extracted by the Unmix model with Min. R^2 and Min. S/N being 0.90 and 4.13, respectively. The residual scale was within ± 3 standard deviation (Fig. S3), which satisfies the operation of the model. More details about the Unmix model can be found elsewhere (Henry 2003, 2007).

Dating of sediment core

The activities of ^{137}Cs, ^{210}Pb, and ^{226}Ra in each sediment sample were measured using an Ortec HPGe GWL series well-type coaxial low-background intrinsic germanium detector. ^{137}Cs was determined by its emissions at 662 keV. ^{210}Pb, ^{226}Ra, and ^{214}Pb (daughter isotope of ^{226}Ra) were measured via its gamma emissions at 46.5, 295, and 352 keV, respectively. ^{210}Pb$_{exe}$ activities were calculated by subtracting ^{226}Ra activities from total ^{210}Pb activities (Wu et al. 2006). The ^{210}Pb$_{exe}$ activities were shown to exponentially decrease with depth (Fig. 1a), indicating a possibility to date the sediment core using the constant initial concentration (CIC) model (Krishnaswamy et al. 1971; Zhang et al. 2013). The average sedimentary rate based on the CIC model was 0.46 cm year^{-1}. The peak value of ^{137}Cs was measured at the depth of 24 cm (Fig. 1b), which was most likely in 1963 due to the large-scale nuclear test world-widely. The average sedimentary rate was 0.47 cm year^{-1} based on ^{137}Cs, which was almost equal to the result of ^{210}Pb$_{exe}$. The similarity from both methods suggested that the dating results were credible. The dating results revealed that the 37-cm sediment core tracked the past 80 years' sedimentary history (1934–2012).
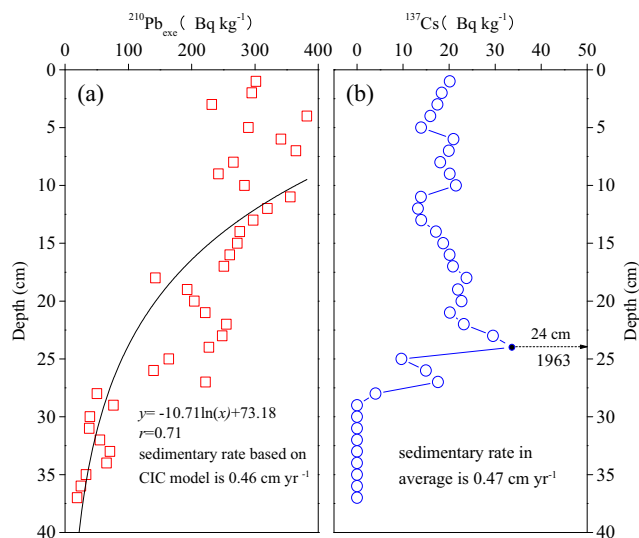
Fig. 1 Depth profiles of ^{210}Pb$_{exe}$ (**a**) and ^{137}Cs activities (**b**) in sediment core from Honghu Lake

Results and discussion

The level of PAHs in sediment core

As shown in Table 1, Phe was the most abundant species with an average of 62.0 ± 32.8 ng g^{-1}, followed by BbF (28.1 ± 13.9 ng g^{-1}), and Fla (26.0 ± 10.9 ng g^{-1}). The total concentrations of 16 PAHs ($\sum_{16}$PAHs) ranged from 93.0 to 431 ng g^{-1}, with an average value of 244 ng g^{-1}. Compared with other studies, the concentrations range of $\sum_{16}$PAHs in

Table 1 Summery of PAH concentrations (ng g^{-1}) in sediment core form Honghu Lake

	Range	Average	SD
Nap	3.47–36.4	15.9	6.50
Acy	0.23–10.3	1.66	2.21
Ace	N.D.–29.8	3.88	7.50
Fl	5.14–27.4	11.5	6.11
Phe	21.9–129	62.0	32.82
Ant	0.66–7.84	3.30	1.95
Fla	8.45–47.5	26.0	10.9
Pyr	6.43–38.4	18.30	7.99
BaA	1.47–12.5	6.02	3.05
Chr	3.77–24.0	13.8	6.92
BbF	7.12–51.9	28.1	13.9
BkF	1.68–19.2	7.86	4.46
BaP	N.D.–15.4	7.92	4.89
IcdP	3.57–30.6	17.6	9.07
DBA	0.79–12.3	4.12	2.68
BghiP	3.18–28.2	16.3	8.58
$\sum_{16}$PAHs	93.0–431	244	95.1

SD standard deviation, *N.D.* not detected

this study was higher than the values reported in Qinghai Lake (11–279 ng g^{-1}) (Wang et al. 2010) and the Nador Lagoon in Morocco (59.0–107.7 ng g^{-1}) (Giuliani et al. 2015), but was lower than those measured in Haizhou Bay (72.5–805 ng g^{-1}) (Zhang et al. 2013), a reservoir in northeast China (243–1004 ng g^{-1}) (Lin et al. 2012), the Lake Lille Lungegårdsvannet in Norway (260–58,360 ng g^{-1}) (Andersson et al. 2014), five lakes in western China (626–1398 ng g^{-1}) (Xu et al. 2014), and the Lake Baiyangdian (97–2404 ng g^{-1}) (Guo et al. 2011).

Source apportionment

The diagnosis ratio method was firstly used to identify the possible PAH sources before the application of receptor models. The diagnostic PAH ratios which exhibited differentiation were the BaA/(BaA + Chr) and IcdP/(IcdP + BghiP) ratios (Fig. S4). The ratios of BaA/(BaA + Chr) > 0.35 and IcdP/(IcdP + BghiP) > 0.5 suggested coal or biomass (wood, grass) burning; the ratios of BaA/(BaA + Chr) < 0.35 and IcdP/(IcdP + BghiP) < 0.5 indicated liquid fossil fuel and petroleum combustion (Yunker et al. 2002). For the ratio of BaA/(BaA + Chr), the values ranged from 0.23 to 0.42, reflecting liquid fossil fuel combustion and coal, grass, or wood combustion. The same results were also found from the ratio of IcdP/(IcdP + BghiP) with the values ranging from 0.49 to 0.55. The diagnosis ratio indicated that PAHs in sediment core of this study were mainly from the liquid fossil fuel combustion and biomass/coal combustion.

PCA-MLR

Based on the principle component and Varimax rotation methods, three factors with the eigenvalue greater than 1 were extracted, and these three factors accounted for 84.8% of the total variances (Table S3). The rotated factor loadings obtained by the PCA-MLR model are shown in Fig. 2a. Factor 1, accounting for 57.5% of variance, was highly loaded on BaA, Chr, BbF, BkF, and IcdP, which indicates diesel combustion (Harrison et al. 1996). In addition, factor 1 was also loaded on Fla, Pyr, DBA, and BghiP, which represent the profile of gasoline engine emission (Larsen and Baker 2003; Wang et al. 2009). Therefore, factor 1 was identified as petroleum combustion. Factor 2 (accounting for 18.7% of the total variance) was dominated by Fl, Phe, and Ant. Nap, Fla, and Pyr also accounted for some loadings in this factor. Phe and Fl are often from coal combustion (Mai et al. 2001; Mai et al. 2003), while Ant is used as the marker of wood combustion source (Harrison et al. 1996). Nap could also originate from incomplete combustion (Simcik et al. 1999). Therefore, factor 2 might be the mixed sources of wood and coal combustion sources. Factor 3 (accounting for 8.67% of the total variance) got high loadings on Acy, Ace, Fl, Phe, and Ant. These low
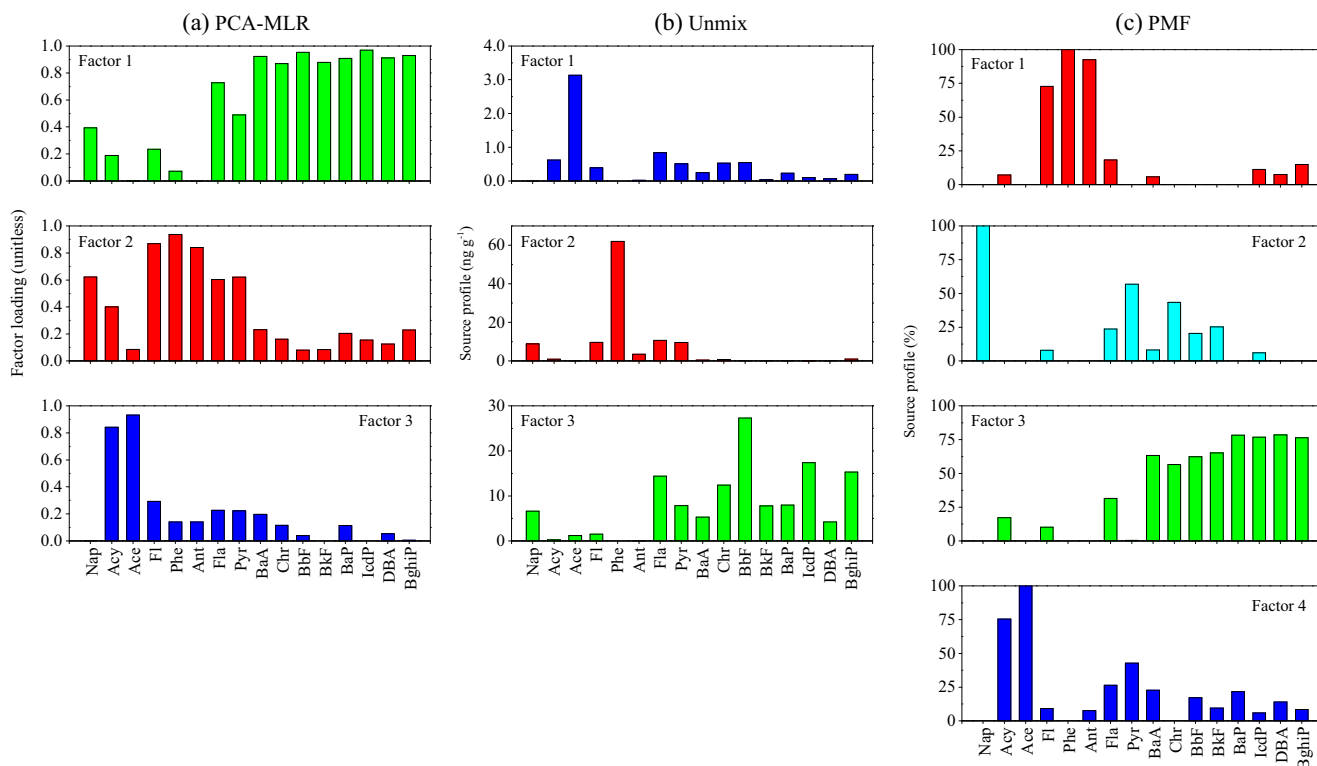
Fig. 2 Source compositions obtained from PCA-MLR (**a**), Unmix (**b**), and PMF (**c**) receptor models

molecular weight PAHs are abundant factions in petrogenic sources such as crude oil and petroleum (Liu et al. 2009; Yu et al. 2015). Therefore, factor 3 was labeled as oil leakage. The calculated average contributions based on MLR were 45.5, 41.4, and 13.1% for petroleum combustion, mixed sources of coal and wood combustion, and oil leakage, respectively.

Unmix

Three sources were extracted by the Unmix model, and the source compositions are shown in Fig. 2b. Ace was the dominating species in factor 1. Acy, Fl, Fla, and Pyr also accounted for some loadings in factor 1. The source profile of factor 1 was similar to factor 3 in PCA-MLR analysis. Thus, factor 1 was identified as oil leakage. Factor 2 was heavily weighted by Phe and moderately influenced by Fl, Fla, and Nap. Consequently, factor 2 was labeled as mixed sources of coal and biomass combustion. Factor 3 was significant influenced by Nap, Fla, Pyr, Chr, BbF, BkF, IcdP, and BghiP, which was similar with factor 1 in PCA-MLR. Therefore, factor 3 represented petroleum combustion. The estimated average contributions were 21.3, 39.5, and 39.2% for petrogenic source, mixed sources, and petroleum combustion, respectively.

PMF

Four factors were identified by the PMF model, and the source profiles are shown in Fig. 2c. Factor 1, which accounted for

31.0% of the $\sum_{16}$PAHs, strongly reflected the variation of Phe and was also influenced by Ant, Fl, and Fla, to some extent. It has been reported that Phe can be identified as the marker of coal combustion sources (Sofowote et al. 2008) and Ant can be used as the tracer of wood combustion sources (Harrison et al. 1996). Therefore, factor 1 indicated the mixed sources of coal and wood combustion. Factor 2 was responsible for 20.9% of the $\sum_{16}$PAHs, which was mainly loaded on Nap and moderately on Pyr, Chr, Fla, BbF, BkF, and BaA. Nap can be derived from sources related to incomplete combustion (Simcik et al. 1999) or oil leakage (Dahle et al. 2003), while Fla and Pyr have been used as markers of coal combustion emission (Kulkarni and Venkataraman 2000; Fang et al. 2006). In addition, BbF, BkF, and Chr are the main PAH components emitted by domestic coal combustion in China (Chen et al. 2005). Therefore, factor 2 indicated contributions from domestic coal combustion. Factor 3, which explained 31.8% of the $\sum_{16}$PAHs, was highly loaded on BaA, BbF, BaP, IcdP, and BghiP. The same profile was also found in diesel and gasoline combustion (Harrison et al. 1996; Mai et al. 2003). Therefore, factor 3 was labeled as petroleum combustion. Factor 4 was predominately weighted on Acy and Ace, and moderately loaded on Pyr, Fla, Ant, and Fl. Acy and Ace are low molecular weight PAHs, which are abundant factions in petrogenic sources such as crude oil and petroleum (Liu et al. 2009; Yu et al. 2015). Pyr, Fla, and Phe are also associated with the contribution of crude oil (Lang et al. 2015). Fishery is one of the most important

functions of the Honghu Lake, and the oil spills from the fishing boat were inevitable. Therefore, factor 4 indicated oil leakage, and this factor accounted for 16.3% of the $\sum_{16}$PAHs.

Comparison of three receptor model results

PCA-MLR, PMF, and Unmix are source unknown receptor models, which do not require the source profile information. These models presume that species with similar variability are clustered together in a minimum number of factors that explain the variability of the whole dataset, or rather that each factor is associated with a source or source type (Larsen and Baker 2003; Yang et al. 2013a). In addition, these three receptor models are factor analysis-based methods. Therefore, they have been widely used in pollutant source apportionment studies due to their convenience. However, these models have their own advantages and disadvantages. For example, PMF is very complicated and time consuming for that the number of factors is unknown and needs further evaluation. By contrast, PCA-MLR and Unmix are relatively simple and easy to operate. To better understand the PAH source apportionment in the sediment core, results from multi-receptor models were applied and compared.

It is recommended that four aspects should be prioritized when comparing the results applying different receptor models. The four aspects include (1) the correlation coefficient between the observed and predicted (O/P) PAH concentrations in a certain model (Larsen and Baker 2003; Yang et al. 2013a), (2) the correlation efficiency between the O/P among the different models (Song et al. 2006; 2008), (3) the source numbers and compositions identified by different models, and (4) contributions of each source to the total concentrations (Cao et al. 2011; Zhang et al. 2012).

Intra-comparison of observed and predicted concentrations by a certain model

The fitting degree between the observed and predicted concentrations of $\sum_{16}$PAHs in a certain model was evaluated by scatter plot as shown in Fig. 3. Significant correlations ($p < 0.01$) between O/P scatter plots were found with r, slop, and intercept ranging from 0.998 to 1.000, 1.00 to 1.02, and − 1.45 to 0.49, respectively. In particular, PMF showed the best fitting degree with almost one-to-one fitting. In addition, high correlation coefficients between observed and predicted concentrations of 16 PAH species were also found with the r ranging from 0.37 to 1.00 (Fig. S5). Pearson correlation is known to be sensitive to the phase in the trend of two variables, and it tells little about the differences in amplitude (Belis et al. 2015). Therefore, another three statistical parameters were
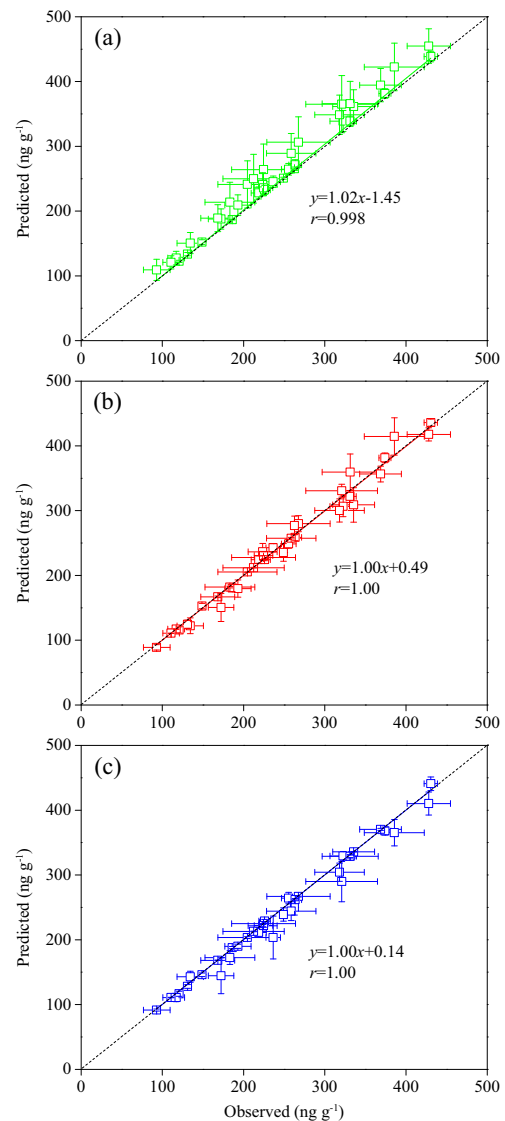

Fig. 3 Fits among the observed and predicted concentrations of $\sum_{16}$PAHs in the sediment core by PCA-MLR (**a**), Unmix (**b**), and PMF (**c**) receptor models

computed to better quantify the differences between solutions reported for O/P data (Table 2): the root mean square error (RMSE), the absolute fractional bias (AFB), and the weighted difference (WD) defined as the following equations, respectively (Cesari et al. 2016):

$$RMSE = \sqrt{\frac{1}{m}\sum_{N=1}^{m}(X_N - Y_N)^2} \tag{2}$$

$$AFB = 2/m \sum_{N=1}^{m} |X_N - Y_N| / (X_N + Y_N) \tag{3}$$

$$WD = 1/m \sum_{N=1}^{m} \frac{|X_N - Y_N|}{\sqrt{S_N^2 + r_N^2}} \tag{4}$$

Table 2 Comparison of observed and predicted PAH concentrations using three different receptor models

Species	PCA-MLR			PMF			Unmix		
	RMSE	AFB	WD	RMSE	AFB	WD	RMSE	AFB	WD
Nap	3.41	0.18	0.54	4.60	0.14	0.53	4.18	0.30	0.71
Acy	0.99	0.37	0.72	0.75	0.46	0.79	0.75	0.33	0.69
Ace	2.26	0.77	0.91	0.85	0.36	0.73	0.98	0.31	0.74
Fl	1.80	0.14	0.66	1.77	0.16	0.71	1.79	0.13	0.65
Phe	9.79	0.14	0.62	10.67	0.01	0.20	10.97	0.15	0.65
Ant	0.95	0.25	0.82	0.94	0.28	0.82	0.97	0.25	0.80
Fla	2.41	0.08	0.48	2.58	0.04	0.38	2.65	0.08	0.52
Pyr	4.15	0.18	0.71	4.40	0.12	0.63	4.40	0.18	0.70
BaA	0.68	0.09	0.59	0.73	0.07	0.50	0.75	0.09	0.56
Chr	3.04	0.17	0.71	3.07	0.14	0.71	3.15	0.19	0.78
BbF	3.82	0.09	0.57	4.18	0.10	0.55	4.22	0.13	0.66
BkF	1.90	0.11	0.62	1.93	0.10	0.53	1.97	0.11	0.62
BaP	1.62	0.23	0.56	1.71	0.26	0.59	1.66	0.31	0.65
IcdP	1.70	0.09	0.50	1.65	0.08	0.47	1.70	0.08	0.48
DBA	0.91	0.13	0.54	0.89	0.10	0.50	0.90	0.11	0.52
BghiP	2.39	0.13	0.61	2.42	0.10	0.52	2.46	0.53	0.62
$\sum_{16}$PAHs	8.97	0.07	0.71	12.10	0.03	0.42	11.94	0.07	0.49

where m is the total number of samples; X_N and Y_N are the observed and predicted PAH concentrations; S_N and r_N represent their uncertainties. RMSE is always used to indicate the spread of the O/P series; the AFB is an indicator of the fitness of the concentrations (accepted range is 0 to 2); the WD is commonly used to test the relationship of the distance between two-variable series considering their uncertainty (the range of acceptability is considered between 0 and 2). Seen from Table 2, RMSE values suggested a certain level of scatter in $\sum_{16}$PAH concentrations (8.83 ± 0.17 ng g^{-1}) for the three models mainly due to Phe (9.21 ± 2.23 ng g^{-1}). WD and AFB were in the acceptable ranges indicating the similarity of amplitude.

Inter-comparison of modeled $\sum_{16}$PAHs within different models

Significant correlations ($p < 0.01$) were also found between the observed and predicted concentrations of $\sum_{16}$PAHs in the inter-comparison. Seen from Fig. 4, the r and slope ranged from 0.98 to 1.00 and 0.96 to 1.02, respectively. The best fitting was found between PMF/Unmix, followed by PCA-MLR/Unmix and PCA-MLR/PMF. Same results were also found in source apportionment for PAHs in atmosphere (Larsen and Baker 2003; Ma et al. 2010), sediments (Zhang et al. 2012), and soil (Yang et al. 2013a). Good correlations between the inter-comparisons indicated that the source apportionment results obtained from these models were comparable.

Source numbers and compositions

Three sources (mixed sources of coal and biomass combustion, petroleum combustion, and oil leakage) were both identified by PCA-MLR and Unmix receptor models as discussed above. The source numbers identified by PCA-MLR is eigenvalue based, while the Unmix model needs mass receptor sample data to generate certain source numbers (i.e., 200~300 samples generate five sources and 2000~3000 samples produce seven sources). In this study, only 37 samples were available and three sources were identified by the Unmix model. As for the PMF model, four factors were apportioned including the three commonly identified sources and the domestic coal combustion. In PMF model analysis, the appropriate numbers of source are co-determined by Q values, scaled residuals, predicted versus observed concentration interpretation, and the physical meaning of factor profiles (Baudic et al. 2016).

To better compare the source compositions, the source profiles/loadings were normalized and exhibited in Fig. 5. The mixed sources were characterized by high loadings on Fl, Phe, and Ant. Petroleum combustion was characterized by high loadings on high molecular weight PAHs (BbF, BkF, BaP, IcdP, DBA, and BghiP), whereas oil leakage source got high loadings on low molecular weight PAHs. The Pearson correlation analysis between the source profiles obtained from different models exhibited significant correlations ($p < 0.01$), with r ranging from 0.51 to 0.68, 0.57 to 0.80, and 0.80 to 0.86 for mixed sources, petroleum combustion, and oil leakage, respectively (Table S4). The results suggested that the source profiles derived from three receptor models agreed with each other.
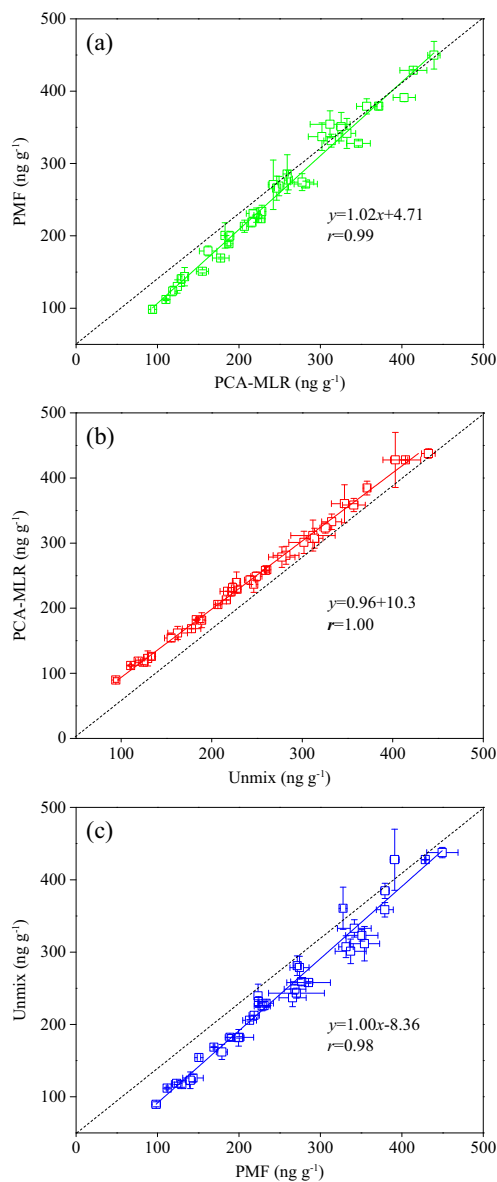
Fig. 4 Inter-comparison of observed and predicted concentrations of $\sum_{16}$PAHs in the sediment core by three different receptor modes. PCA-MLR vs PMF (**a**),Unmix vs PCA-MLR (**b**), and PMF vs Unmix (**c**)
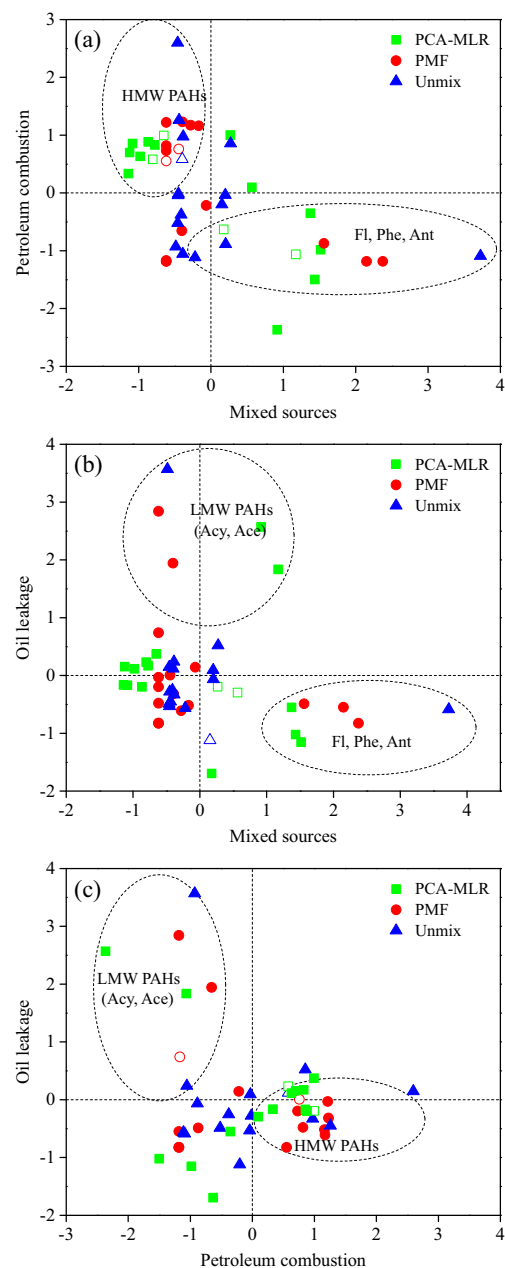

Fig. 5 Scatter plots of normalized factor loadings or profiles of identified possible PAH sources by three different models. Mixed sources vs petroleum combustion (**a**), mixed sources vs oil leakage (**b**), and petroleum combustion vs oil leakage (**c**)

Source contributions

Figure 6 exhibited the average contributions of each identified source to the $\sum_{16}$PAHs by different receptor models. For the average contributions of three common sources, petroleum combustion was highest (31.8 to 45.5%), followed by mixed sources (31.0 to 41.4%) and oil leakage (13.1 to 21.3%). The recent studies indicated that biomass burning and coal combustion were the main PAH sources in surface sediments in China (Table 3). However, the source contributions of mixed sources derived from PCA-MLR and Unmix in this study were different from previous studies. For example, Xu et al. (2006) and Zhang et al. (2007) found that coal combustion and biomass burning were the dominant PAH sources in

China. The source apportionment results from the PMF model indicated that biomass burning and coal combustion contributed most (50.9%) to PAHs in the sediment core. The average contribution of each source to $\sum_{16}$PAHs did not convey detailed information of source contribution in each sample/layer. Therefore, the historical distributions of each identified PAH source contribution estimated by the three receptor models were as shown in Fig. 7. It should be noted that the mixed sources in the PMF model included biomass burning and coal combustion.

Fig. 6 Average contribution of each source to $\sum_{16}$PAHs apportioned from PCA-MLR (**a**), Unmix receptor models (**b**), and PMF (**c**) receptor models
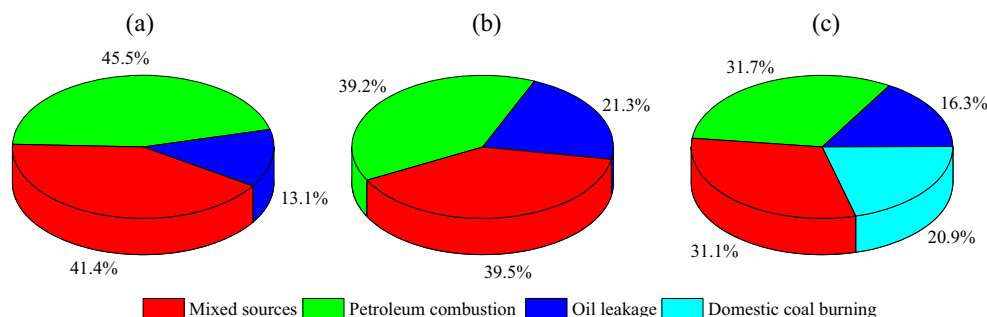
Seen from Fig. 7, before 1949, the temporal variations of three sources deduced from three models were similar. In this period, the mixed source contributions (ng g^{-1}) decreased from 131 ± 26.4 to 70.1 ± 13.9 ng g^{-1} and petroleum combustion increased from 4.44 ± 13.5 to 23.5 ± 8.06 ng g^{-1}. Despite that the mixed sources showed an opposite trend to petroleum combustion, the mixed sources still contributed most (69.8 ± 12.4%) to $\sum_{16}$PAHs in sediment of Honghu Lake, followed by oil leakage (19.5 ± 6.28%) and petroleum combustion (10.7 ± 8.26%) in this period. From 1949 to 1960, the source contributions (ng g^{-1}) of mixed sources and petroleum combustion dramatically increased, while the percentage contributions (%) of mixed sources decreased. In this period, mixed sources still contributed most (62.6 ± 13.9%) to $\sum_{16}$PAHs. From 1960 to 1978, the variations of source contributions were complex due to social activities. The percentage contributions of petroleum combustion derived from PCA-MLR (61.7 ± 9.93%) and Unmix (59.8 ± 11.6%) were higher than that derived from PMF (41.5 ± 8.03%) during this period. From 1978 to 1995, the mixed sources and petroleum combustion both exhibited an increasing trend and petroleum combustion was still the dominant PAH source (> 50%) calculated by PCA-MLR and Unmix models. From 1997 to 2005, both the concentration and percentage contributions of mixed sources and petroleum combustion source decreased significantly due to the floods and the pollution control measurements. Compared with the temporal variation calculated

from PCA-MLR and Unmix models, the PMF-derived variation was relatively stable without an outlier in this period. From 2005 to now, the contributions of mixed sources and petroleum combustion increased again due to another round of urbanization and industrialization (Xu et al. 2006; Zhang et al. 2007).

For oil leakage source, it exhibited a relative stable temporal variation except three peak values apportioned from Unmix and PCA-MLR that occurred in 1997, 2006, and 2012, which accounted for 17.5–66.4, 54.1–92.0, and 26.8–73.6% to $\sum_{16}$PAHs, respectively. Larsen and Baker (2003) suggested that the PMF model employed uncertain files to down-weight the outlying variables and it allowed for additional dimensions affecting the measured concentrations not explained by the sources alone, such as weather, additional transient source, or sampling artifacts. Therefore, the temporal distribution of oil leakage deduced from the PMF model was stable compared with the PCA-MLR and Unmix models.

Given the fact that biomass burning and coal combustion are the main PAH sources in surface sediments in China (Table 3), the source contributions of petroleum combustion calculated from PCA-MLR and Unmix were higher than 50% during some periods (i.e., 1960 to 1978). While the results from the PMF model agreed with the real situation that coal combustion and biomass burning are the dominant PAHs in China. The historical statistical data of coal consumption and domestic coal combustion from the PMF model also

Table 3 The published papers concerning PAH source contributions (%) in surface sediment in China

| Areas	Sampling year	Traffic-related emission	Coal combustion	Biomass burning	Petrogenic source	References
Taihu Lake, China	2010	53.6–54.3	23.8–28.8	11.9–16.0	–	(Zhang et al. 2012)
Baiyangdian, China	2008	36	64	–	–	(Liu et al. 2010)
Chaohu Lake, China	2011	41.1	44.0	14.5	–	(Li et al. 2014)
Fenhe reservoir, China	2010	45.0	35.0	–	–	(Li et al. 2012)
Rizhao offshore area, China	2007	15.0	75.7	–	9.3	(Xue et al. 2010)
Dahuofang Reservoir, Northeast China	2010	10.0	31.0	21.0	16.0	(Lin et al. 2013)
Yellow River, China	2005	25.1–36.7	34.0–41.6	29.2–33.2	–	(Feng et al. 2014)
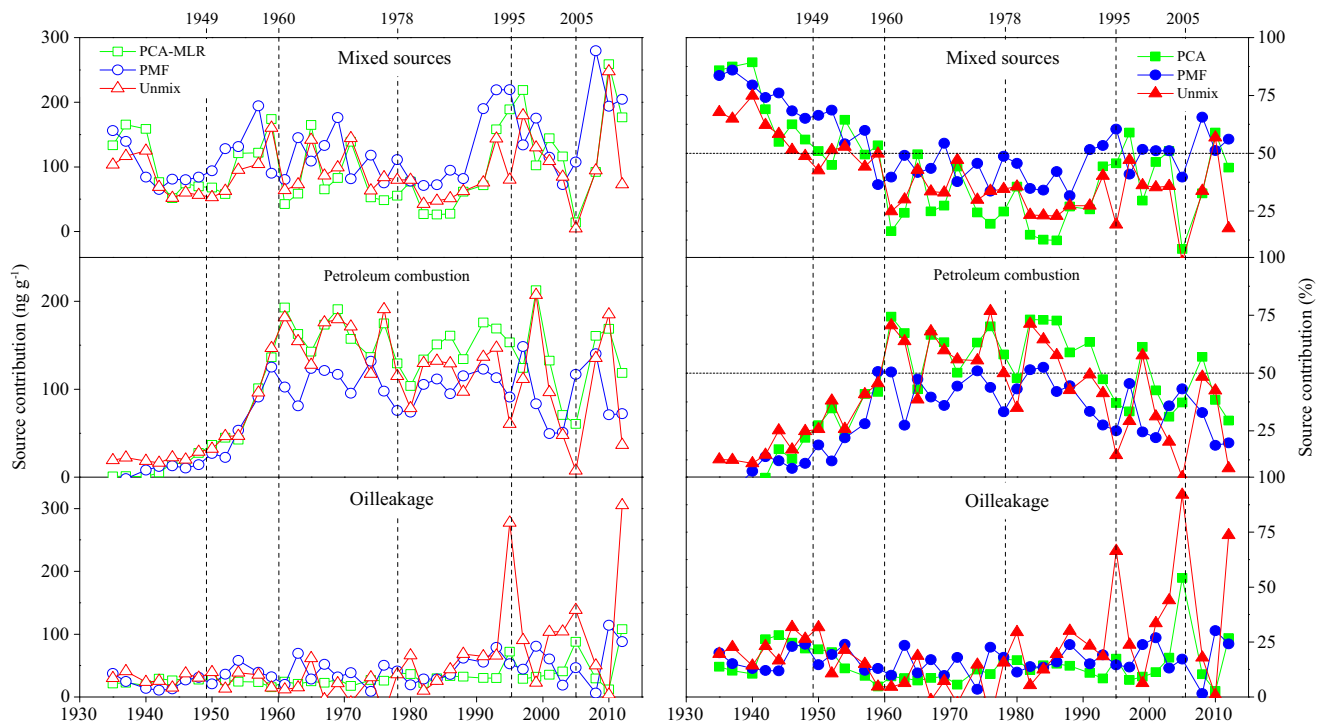
Fig. 7 Historical variation of concentration contribution (left panel) and percentile contribution (right panel) of different sources identified by three receptor models

correlated well with each other (Fig. S6). Therefore, we think that the source apportionment results employing the PMF model were most reasonable due to the following reasons: (1) best fits between the observed and predicted PAH concentrations, (2) the segregation of the domestic coal combustion sources, and (3) the reasonable temporal distribution of source contributions as discussed above.

Suggestion to source apportionment studies

The identification and quantification of the sources of pollutants at the receptor samples employing the receptor models are mathematical or statistical procedures. In view of mathematical or statistical procedures, the source apportionment results from three different receptor models were acceptable. However, the source apportionment is more than just mathematics; the source apportionment results should be reasonable. In this study, the real situation that coal and biomass combustion still contributed most to PAHs in the environment at present in China, not to mention several decades ago. Therefore, the PMF model was thought to be more reasonable. In source apportionment studies concerning temporal variation, we suggested that the correlation between the statistical data (i.e., the energy consumption) and the corresponding historical source contribution should be checked. In other source apportionment studies related to spatial distribution, we suggested that the relationship between the geographic

location of pollution source and the spatial distribution of source contributions should be taken into account.

Conclusion

In this paper, the source apportionment of 16 US EPA priority PAHs in the sediment core from the Honghu Lake employing three different receptor models was carried out. The four aspects including the observed and predicated PAH concentrations in a certain model or different model, source numbers and compositions, and source contributions were prioritized in the comparison study. The results suggested that PMF was more reasonable compared with PCA-MLR and Unmix models. The high-resolution temporal distribution of source contributions indicated that biomass burning and coal combustion were the main sources before 1960 and after 1993, while petroleum combustion increased from the bottom sediment to the surface. Suggestions were also made for source apportionment studies concerning the temporal/spatial distribution of pollutants.

References

Andersson M, Klug M, Eggen OA, Ottesen RT (2014) Polycyclic aromatic hydrocarbons (PAHs) in sediments from lake Lille Lungegårdsvannet in Bergen, western Norway; appraising pollution sources from the urban history. Sci Total Environ 470–471:1160–1172. https://doi.org/10.1016/j.scitotenv.2013.10.086

Baudic A, Gros V, Sauvage S, Locoge N, Sanchez O, Sarda-Estève R, Kalogridis C, Petit J-E, Bonnaire N, Baisnée D, Favez O, Albinet A, Sciare J, Bonsang B (2016) Seasonal variability and source apportionment of volatile organic compounds (VOCs) in the Paris megacity (France). Atmospheric Chem Phys 16:11961–11989. https://doi.org/10.5194/acp-16-11961-2016

Belis CA, Pernigotti D, Karagulian F, Pirovano G, Larsen BR, Gerboles M, Hopke PK (2015) A new methodology to assess the performance and uncertainty of source apportionment models in intercomparison exercises. Atmos Environ 119:35–44. https://doi.org/10.1016/j.atmosenv.2015.08.002

Bzdusek PA, Christensen ER, Li A, Zou Q (2004) Source apportionment of sediment PAHs in Lake Calumet, Chicago: application of factor analysis with nonnegative constraints. Environ Sci Technol 38:97–103. https://doi.org/10.1021/es034842k

Cao Q, Wang H, Chen G (2011) Source apportionment of PAHs using two mathematical models for mangrove sediments in Shantou coastal zone, China. Estuar Coasts 34:950–960. https://doi.org/10.1007/s12237-011-9397-3

Cesari D, Amato F, Pandolfi M, Alastuey A, Querol X, Contini D (2016) An inter-comparison of PM10 source apportionment using PCA and PMF receptor models in three European sites. Environ Sci Pollut Res 23:15133–15148. https://doi.org/10.1007/s11356-016-6599-z

Chen Y, Sheng G, Bi X, Feng Y, Mai B, Fu J (2005) Emission factors for carbonaceous particles and polycyclic aromatic hydrocarbons from residential coal combustion in China. Environ Sci Technol 39:1861–1867. https://doi.org/10.1021/es0493650

Dahle S, Savinov VM, Matishov GG, Evenset A, Næs K (2003) Polycyclic aromatic hydrocarbons (PAHs) in bottom sediments of the Kara Sea shelf, Gulf of Ob and Yenisei Bay. Sci Total Environ 306:57–71. https://doi.org/10.1016/S0048-9697(02)00484-9

Fang G, Wu Y, Chang C, Ho T (2006) RETRACTED: a study of polycyclic aromatic hydrocarbons concentrations and source identifications by methods of diagnostic ratio and principal component analysis at Taichung chemical Harbor near Taiwan Strait. Chemosphere 64:1233–1242. https://doi.org/10.1016/j.chemosphere.2005.11.031

Feng C, Xia X, Shen Z, Zhou Z (2007) Distribution and sources of polycyclic aromatic hydrocarbons in Wuhan section of the Yangtze River, China. Environ Monit Assess 133:447–458. https://doi.org/10.1007/s10661-006-9599-5

Feng J, Li X, Guo W, Liu S, Ren X, Sun J (2014) Potential source apportionment of polycyclic aromatic hydrocarbons in surface sediments from the middle and lower reaches of the Yellow River, China. Environ Sci Pollut Res 21:11447–11456. https://doi.org/10.1007/s11356-014-3051-0

Giuliani S, Piazza R, El Moumni B, Polo FP, Vecchiato M, Romano S, Zambon S, Frignani M, Bellucci LG (2015) Recognizing different impacts of human and natural sources on the spatial distribution and temporal trends of PAHs and PCBs (including PCB-11) in sediments of the Nador Lagoon (Morocco). Sci Total Environ 526: 346–357. https://doi.org/10.1016/j.scitotenv.2015.04.057

Grimalt JO, van Drooge BL, Ribes A, Fernández P, Appleby P (2004) Polycyclic aromatic hydrocarbon composition in soils and sediments of high altitude lakes. Environ Pollut 131:13–24. https://doi.org/10.1016/j.envpol.2004.02.024

Guo J, Wu F, Luo X, Liang Z, Liao H, Zhang R, Li W, Zhao X, Chen S, Mai B (2010) Anthropogenic input of polycyclic aromatic hydrocarbons into five lakes in Western China. Environ Pollut 158:2175–2180. https://doi.org/10.1016/j.envpol.2010.02.018

Guo W, Pei Y, Yang Z, Chen H (2011) Historical changes in polycyclic aromatic hydrocarbons (PAHs) input in Lake Baiyangdian related to regional socio-economic development. J Hazard Mater 187:441–449. https://doi.org/10.1016/j.jhazmat.2011.01.052

Guo Z, Lin T, Zhang G, Yang Z, Fang M (2006) High-resolution depositional records of polycyclic aromatic hydrocarbons in the central continental shelf mud of the East China Sea. Environ Sci Technol 40:5304–5311. https://doi.org/10.1021/es060878b

Harrison RM, Smith DJT, Luhana L (1996) Source apportionment of atmospheric polycyclic aromatic hydrocarbons collected from an urban location in Birmingham, U.K. Environ Sci Technol 30:825–832. https://doi.org/10.1021/es950252d

Henry RC (1997) History and fundamentals of multivariate air quality receptor models. Chemom Intell Lab Syst 37:37–42. https://doi.org/10.1016/S0169-7439(96)00048-2

Henry RC (2003) Multivariate receptor modeling by N-dimensional edge detection. Chemom Intell Lab Syst 65:179–189. https://doi.org/10.1016/S0169-7439(02)00108-9

Henry RC (2007) EPA Unmix 6.0 fundamentals and user guide. US Environmental Protection Agency. https://www.epa.gov/air-research/unmix-60-model-environmental-data-analyses

Hopke PK (2003) Recent developments in receptor modeling. J Chemom 17:255–265. https://doi.org/10.1002/cem.796

Hu T, Zhang J, Ye C, Zhang L, Xing X, Zhang Y, Wang Y, Sun W, Qi S, Zhang Q (2017) Status, source and health risk assessment of polycyclic aromatic hydrocarbons (PAHs) in soil from the water-level-fluctuation zone of the Three Gorges Reservoir, China. J Geochem Explor 172:20–28. https://doi.org/10.1016/j.gexplo.2016.09.012

Huang W, Wang Z, Yan W (2012) Distribution and sources of polycyclic aromatic hydrocarbons (PAHs) in sediments from Zhanjiang Bay and Leizhou Bay, South China. Mar Pollut Bull 64:1962–1969. https://doi.org/10.1016/j.marpolbul.2012.05.023

Krishnaswamy S, Lal D, Martin JM, Meybeck M (1971) Geochronology of lake sediments. Earth Planet Sci Lett 11:407–414. https://doi.org/10.1016/0012-821X(71)90202-0

Kulkarni P, Venkataraman C (2000) Atmospheric polycyclic aromatic hydrocarbons in Mumbai, India. Atmos Environ 34:2785–2790. https://doi.org/10.1016/S1352-2310(99)00312-X

Lang Y, Li G, Wang X, Peng P, Bai J (2015) Combination of Unmix and positive matrix factorization model identifying contributions to carcinogenicity and mutagenicity for polycyclic aromatic hydrocarbons sources in Liaohe delta reed wetland soils, China. Chemosphere 120:431–437. https://doi.org/10.1016/j.chemosphere.2014.08.048

Lang Y, Yang W (2013) Source apportionment of PAHs using Unmix model for Yantai costal surface sediments, China. Bull Environ Contam Toxicol 92:30–35. https://doi.org/10.1007/s00128-013-1164-7

Larsen RK, Baker JE (2003) Source apportionment of polycyclic aromatic hydrocarbons in the urban atmosphere: a comparison of three methods. Environ Sci Technol 37:1873–1881. https://doi.org/10.1021/es0206184

Li C, Huo S, Yu Z, Xi B, Zeng X, Wu F (2014) Spatial distribution, potential risk assessment, and source apportionment of polycyclic aromatic hydrocarbons (PAHs) in sediments of Lake Chaohu, China. Environ Sci Pollut Res 21:12028–12039. https://doi.org/10.1007/s11356-014-3137-8

Li W, Tian Y, Shi G, Guo C, Li X, Feng Y (2012) Concentrations and sources of PAHs in surface sediments of the Fenhe reservoir and watershed, China. Ecotoxicol Environ Saf 75:198–206. https://doi.org/10.1016/j.ecoenv.2011.08.021

Lin T, Qin Y, Zheng B, Li Y, Chen Y, Guo Z (2013) Source apportionment of polycyclic aromatic hydrocarbons in the Dahuofang Reservoir, Northeast China. Environ Monit Assess 185:945–953. https://doi.org/10.1007/s10661-012-2605-1

Lin T, Qin Y, Zheng B, Li Y, Zhang L, Guo Z (2012) Sedimentary record of polycyclic aromatic hydrocarbons in a reservoir in Northeast China. Environ Pollut 163:256–260. https://doi.org/10.1016/j.envpol.2012.01.005

Liu L, Wang J, Wei G, Jiang Y, Wong CS, Zeng E (2012) Sediment records of polycyclic aromatic hydrocarbons (PAHs) in the continental shelf of China: implications for evolving anthropogenic impacts. Environ Sci Technol 46:6497–6504. https://doi.org/10.1021/es300474z

Liu X, Xu M, Yang Z, Sun T, Cui B, Wang L, Wu D (2010) Sources and risk of polycyclic aromatic hydrocarbons in Baiyangdian Lake, North China. J Environ Sci Health Part A 45:413–420. https://doi.org/10.1080/10934520903540588

Liu Y, Chen L, Huang Q, Li W, Tang Y, Zhao J (2009) Source apportionment of polycyclic aromatic hydrocarbons (PAHs) in surface sediments of the Huangpu River, Shanghai, China. Sci Total Environ 407:2931–2938. https://doi.org/10.1016/j.scitotenv.2008.12.046

Ma W, Li Y, Qi H, Sun D, Liu L, Wang D (2010) Seasonal variations of sources of polycyclic aromatic hydrocarbons (PAHs) to a northeastern urban city, China. Chemosphere 79:441–447. https://doi.org/10.1016/j.chemosphere.2010.01.048

Mai B, Fu J, Zhang G, Lin Z, Min Y, Sheng G, Wang X (2001) Polycyclic aromatic hydrocarbons in sediments from the Pearl river and estuary, China: spatial and temporal distribution and sources. Appl Geochem 16:1429–1445. https://doi.org/10.1016/S0883-2927(01)00050-6

Mai B, Qi S, Zeng EY, Fu J, Sheng G, Peng P, Wang Z (2003) Distribution of polycyclic aromatic hydrocarbons in the coastal region off Macao, China: assessment of input sources and transport pathways using compositional analysis. Environ Sci Technol 37:4855–4863. https://doi.org/10.1021/es034514k

Malik A, Verma P, Singh AK, Singh KP (2011) Distribution of polycyclic aromatic hydrocarbons in water and bed sediments of the Gomti River, India. Environ Monit Assess 172:529–545. https://doi.org/10.1007/s10661-010-1352-4

Micić V, Kruge MA, Köster J, Hofmann T (2011) Natural, anthropogenic and fossil organic matter in river sediments and suspended particulate matter: a multi-molecular marker approach. Sci Total Environ 409:905–919. https://doi.org/10.1016/j.scitotenv.2010.11.009

Readman J, Fillmann G, Tolosa I, Bartocci J, Villeneuve J-P, Catinni C, Mee L (2002) Petroleum and PAH contamination of the Black Sea. Mar Pollut Bull 44:48–62. https://doi.org/10.1016/S0025-326X(01)00189-8

Shi G, Li X, Feng Y, Wang Y, Wu J, Li J, Zhu T (2009) Combined source apportionment, using positive matrix factorization–chemical mass balance and principal component analysis/multiple linear regression–chemical mass balance models. Atmos Environ 43:2929–2937. https://doi.org/10.1016/j.atmosenv.2009.02.054

Simcik MF, Eisenreich SJ, Lioy PJ (1999) Source apportionment and source/sink relationships of PAHs in the coastal atmosphere of Chicago and Lake Michigan. Atmos Environ 33:5071–5079. https://doi.org/10.1016/S1352-2310(99)00233-2

Sofowote UM, Hung H, Rastogi AK, Westgate JN, Deluca PF, Su Y, McCarry BE (2011) Assessing the long-range transport of PAH to a sub-Arctic site using positive matrix factorization and potential source contribution function. Atmos Environ 45:967–976. https://doi.org/10.1016/j.atmosenv.2010.11.005

Sofowote UM, McCarry BE, Marvin CH (2008) Source apportionment of PAH in Hamilton harbour suspended sediments: comparison of two factor analysis methods. Environ Sci Technol 42:6007–6014. https://doi.org/10.1021/es800219z

Song Y, Dai W, Shao M, Liu Y, Lu S, Kuster W, Goldan P (2008) 1987) Comparison of receptor models for source apportionment of volatile organic compounds in Beijing, China. Environ Pollut Barking Essex 156:174–183. https://doi.org/10.1016/j.envpol.2007.12.014

Song Y, Xie S, Zhang Y, Zeng L, Salmon LG, Zheng M (2006) Source apportionment of PM2.5 in Beijing using principal component analysis/absolute principal component scores and UNMIX. Sci Total Environ 372:278–286. https://doi.org/10.1016/j.scitotenv.2006.08.041

Stout SA, Graan TP (2010) Quantitative source apportionment of PAHs in sediments of Little Menomonee River, Wisconsin: weathered creosote versus urban background. Environ Sci Technol 44:2932–2939. https://doi.org/10.1021/es903353z

USEPA (2008) EPA positive matrix factorization (PMF) 3.0 fundamentals & user guide. US Environmental Protection Agency. https://www.epa.gov/air-research/positive-matrix-factorization-model-environmental-data-analyses

Wang D, Yang M, Jia H, Zhou L, Li Y (2009) Polycyclic aromatic hydrocarbons in urban street dust and surface soil: comparisons of concentration, profile, and source. Arch Environ Contam Toxicol 56:173–180. https://doi.org/10.1007/s00244-008-9182-x

Wang X, Yang H, Gong P, Zhao X, Wu G, Turner S, Yao T (2010) One century sedimentary records of polycyclic aromatic hydrocarbons, mercury and trace elements in the Qinghai Lake, Tibetan Plateau. Environ Pollut 158:3065–3070. https://doi.org/10.1016/j.envpol.2010.06.034

Wu Y, Wang S, Hou X (2006) Chronology of Holocene lacustrine sediments in Co Ngoin, central Tibetan Plateau. Sci China Ser Earth Sci 49:991–1001. https://doi.org/10.1007/s11430-006-0991-3

Xu J, Guo J, Liu G, Shi G, Guo C, Zhang Y, Feng Y (2014) Historical trends of concentrations, source contributions and toxicities for PAHs in dated sediment cores from five lakes in western China. Sci Total Environ 470–471:519–526. https://doi.org/10.1016/j.scitotenv.2013.10.022

Xu J, Peng X, Guo C, Xu J, Lin H, Shi G, Lv J, Zhang Y, Feng Y, Tysklind M (2016) Sediment PAH source apportionment in the Liaohe River using the ME2 approach: a comparison to the PMF model. Sci Total Environ 553:164–171. https://doi.org/10.1016/j.scitotenv.2016.02.062

Xu S, Liu W, Tao S (2006) Emission of polycyclic aromatic hydrocarbons in China. Environ Sci Technol 40:702–708. https://doi.org/10.1021/es0517062

Xue L, Lang Y, Liu A, Liu J (2010) Application of CMB model for source apportionment of polycyclic aromatic hydrocarbons (PAHs) in coastal surface sediments from Rizhao offshore area, China. Environ Monit Assess 163:57–65. https://doi.org/10.1007/s10661-009-0816-x

Yang B, Zhou L, Xue N, Li F, Li Y, Vogt RD, Cong X, Yan Y, Liu B (2013a) Source apportionment of polycyclic aromatic hydrocarbons in soils of Huanghuai Plain, China: comparison of three receptor models. Sci Total Environ 443:31–39. https://doi.org/10.1016/j.scitotenv.2012.10.094

Yang D, Qi S, Zhang Y, Xing X, Liu H, Qu C, Liu J, Li F (2013b) Levels, sources and potential risks of polycyclic aromatic hydrocarbons (PAHs) in multimedia environment along the Jinjiang River mainstream to Quanzhou Bay, China. Mar Pollut Bull 76:298–306. https://doi.org/10.1016/j.marpolbul.2013.08.016

Yu W, Liu R, Wang J, Xu F, Shen Z (2015) Source apportionment of PAHs in surface sediments using positive matrix factorization combined with GIS for the estuarine area of the Yangtze River, China. Chemosphere 134:263–271. https://doi.org/10.1016/j.chemosphere.2015.04.049

Yunker MB, Macdonald RW, Vingarzan R, Mitchell RH, Goyette D, Sylvestre S (2002) PAHs in the Fraser River basin: a critical appraisal of PAH ratios as indicators of PAH source and composition. Org Geochem 33:489–515. https://doi.org/10.1016/S0146-6380(02)00002-5

Zakaria MP, Takada H, Tsutsumi S, Ohno K, Yamada J, Kouno E, Kumata H (2002) Distribution of polycyclic aromatic hydrocarbons (PAHs) in rivers and estuaries in Malaysia: a widespread input of petrogenic PAHs. Environ Sci Technol 36:1907–1918

Zhang R, Zhang F, Zhang T (2013) Sedimentary records of PAHs in a sediment core from tidal flat of Haizhou Bay, China. Sci Total Environ 450–451:280–288. https://doi.org/10.1016/j.scitotenv.2013.02.029

Zhang Y, Guo CS, Xu J, Tian YZ, Shi GL, Feng YC (2012) Potential source contributions and risk assessment of PAHs in sediments from Taihu Lake, China: comparison of three receptor models. Water Res 46:3065–3073. https://doi.org/10.1016/j.watres.2012.03.006

Zhang Y, Tao S, Cao J, Coveney RM (2007) Emission of polycyclic aromatic hydrocarbons in China by county. Environ Sci Technol 41:683–687. https://doi.org/10.1021/es061545h